Finally Fig. 6.26 gives the subtracted saturated absorption spectrum for Rb starting from the $F = 2$ ground state. Again the prominent lines are the ossover lines $[\nu(F' = 1)+\nu(F' = 3)]/2$ and $[\nu(F' = 2)+\nu(F' = 3)]/2$; e $\nu(F' = 3)$ line is also evident. The location of the other expected lines indicated.

As is evident from the data the saturated absorption lines are very sharp. ius instead of sweeping the laser frequency one can use a servo circuit keep the laser frequency fixed on one of the lines (actually on its slope), aching a stability of $\pm$ few megahertz, in absolute terms.

7. REFERENCES

U. Condon and G. H. Shortley, *The Theory of Atomic Spectra*, Cambridge Univ. Press, Cambridge, UK, 1951. This is one of the most complete theoretical treatments on atomic spectroscopy, but at an advanced level.

E. White, *Introduction to Atomic Spectra*, McGraw-Hill, New York, 1934. This book contains extensive data on atomic spectra, and the treatment of the theory is based on the semiclassical approach of the vector model.

Kuhn, *Atomic Spectra*, Longman's, London, 1962. A good book on a slightly more advanced level than White's book referred to above.

Tolansky, *High Resolution Spectroscopy*, Methuen, London, 1947. A very comprehensive and clear treatise on the instruments and techniques of high-resolution spectroscopy.

Kopferman, *Nuclear Moments*, Academic Press, New York, 1958. This book contains a very complete discussion of atomic hyperfine structure, of analysis methods, and of the conclusions obtained from it.

Demtröeder, *Laser Spectroscopy*, 2nd ed., Springer-Verlag, Berlin, 1996. A very comprehensive and up-to-date coverage of the field.

CHAPTER 7

Magnetic Resonance Experiments

7.1. INTRODUCTION

We saw in the previous chapter that when an atom (or a nucleus), with angular momentum **L** (or **I**), different from 0, is placed in a magnetic field **B** the states that correspond to different values of the quantum number m acquire an additional energy

$$\Delta E = \frac{\mu}{L} Bm. \tag{7.1}$$

Here μ is the "magnetic moment" of the atom or nucleus. When electrons are involved, μ is on the order of the Bohr magneton μ_B while for nuclei μ is on the order of the nuclear magneton, μ_N. In convenient units

$$\begin{aligned} \mu_B/h &= 14.01 \quad \text{GHz/T} \\ \mu_N/h = (\mu_B/h)/1836 &= 7.62 \quad \text{MHz/T}. \end{aligned} \tag{7.2}$$

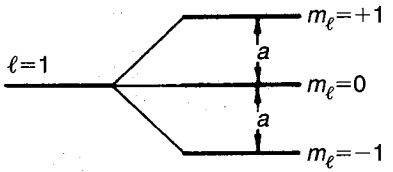

FIGURE 7.1 Splitting of an energy level with $l = 1$ into three components when placed in a magnetic field.

In Fig. 7.1 is shown the splitting of an energy state with $l = 1$ into its three sublevels. As discussed in Chapter 6, in optical spectroscopy we do not observe the spontaneous transitions (labeled a in the figure) between sublevels with different m, because they do not satisfy the selection rule $\Delta l = \pm 1$. Instead the splitting of a level is observed through the small difference in the frequency of the radiation emitted in the transitions between widely distant levels (with $\Delta l = \pm 1$). It is clear that if we could directly measure the frequency corresponding to a transition between the m sublevels of the same state, a much more precise knowledge of the energy splitting would be obtained.

The selection rule $\Delta l = \pm 1$ is applicable to electric-dipole radiation; however, transitions with $\Delta l = 0$, $\Delta m = \pm 1$ do occur when *magnetic-dipole* radiation is emitted, but the probability for such a transition is reduced by a factor[1] $(v/c)^2$ from the case of an electric dipole transition. We therefore conclude that spontaneous transitions with $\Delta l = 0$, $\Delta m = \pm 1$ will be very rare, especially if the system can preferentially return to its ground state (lowest energy state) by a $\Delta l = \pm 1$ transition. On the other hand, in the presence of an electromagnetic field, *induced* transitions have a probability of occurring if the frequency of the field is equal (or at least fairly close) to the energy difference between the two levels; induced transitions toward higher or lower energy states are equally probable. Further, the transition probability is proportional to the square of the strength of the electromagnetic field (that is, the total number of quanta) so that if a sufficiently strong radiofrequency magnetic field (of frequency ν_0) is available, magnetic-dipole transitions should take place.

This fact is, of course, central to the operation of the laser discussed in Section 4.1. In that case the atomic state has an electric-dipole moment and

[1]For atomic systems v is on the order of the velocity in a Bohr orbit, namely, $(v/c)^2 \approx 5 \times 10^{-6}$.

electric-dipole transitions are induced by the external electric field (at the optical frequency) of the laser beam.

By referring to Eq. (7.2) we see that for a 1-T magnetic field the energy splitting of either nuclei or electrons falls in the range of frequencies that can be easily generated. It is also of interest to estimate the magnitude of the *radiofrequency* (or microwave) magnetizing field, which we will designate by H, to distinguish it from the static magnetic (induction) field B; in vacuum $B = \mu_0 H$. An H field of magnitude $10^3/4\pi$ A/m (equivalent to a B field of 10^{-4} T = 1 G) corresponds to an energy flow of

$$\langle S \rangle = \frac{1}{2}\sqrt{\frac{\mu_0}{\epsilon_0}}\,H^2 = \frac{1}{2}\sqrt{\frac{4\pi \times 10^{-7}}{8.85 \times 10^{-12}}} \times \left(\frac{10^3}{4\pi}\right)^2 \approx 2.35 \times 10^2 \frac{\text{W}}{\text{cm}^2}, \tag{7.3}$$

which can be easily generated. Calculation shows that this field strength is adequate for inducing transitions. Finally we must be able to detect the fact that a transition took place; this may be done in several ways and is one of the distinguishing factors between the various types of magnetic resonance experiments.

For example, in the first magnetic resonance experiment, performed by I. I. Rabi and collaborators in 1939, a beam of atoms having $J = \frac{1}{2}$ was passed in succession through two very inhomogeneous magnets A and B shown in Fig. 7.2. A homogeneous magnetic field existed in the intermediate region C where a radiofrequency (RF) field was applied. If a transition took place in region C from a state $m = +\frac{1}{2}$ to $m = -\frac{1}{2}$, that particular atom was deflected in an opposite direction in field B and thus missed the detector. Hence, resonance was detected by a decrease in beam current when the frequency of the RF field was the appropriate one for the magnetic field strength in C.

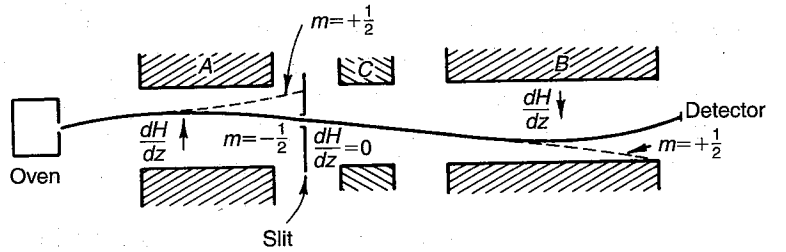

FIGURE 7.2 The atomic beam arrangement of I. I. Rabi and collaborators used to detect magnetic resonance transitions in atomic energy levels.

Another method for detecting the occurrence of resonance is to observe
e absorption of energy from the radiofrequency field when transitions
ward higher energy levels take place. This technique is used in most
uclear magnetic resonance (NMR) experiments and in electron magnetic
sonance (called "electron spin resonance," ESR) experiments. In exper-
nents with atomic vapors or transparent materials it is possible to detect
e magnetic resonance effect by changes in the polarization of the atomic
diation ($\Delta m \neq 0$) or by selective absorption effects.

Apart from its intrinsic interest as a way of inducing transitions between
e energy sublevels of atoms or nuclei, magnetic resonance has become
important tool of physics. The atomic beam experiments of Rabi and
s coworkers led to very precise measurements of the hyperfine structure
atomic systems and thus to accurate values of the nuclear moments. In a
uclear magnetic resonance experiment transitions are induced between
e sublevels of a nucleus placed in an external magnetic field. However,
e atom to which the nucleus belongs must have $J = 0$ (diamagnetic
aterial), since otherwise the nuclear spin would be coupled to J and the
rge electronic magnetic moment would mask the effect. By means of
ch experiments, nuclear magnetic moments are measured directly and to
high accuracy.

The NMR signal depends not only on the nucleus under study but also on
e environment in which the nucleus finds itself. In fact the observation of
uclear magnetic resonance in solids and liquids depends on the relaxation
the nuclear spins through their interaction with the lattice. Thus, nuclear
agnetic resonance studies have yielded a very large amount of information
the properties of many materials in the solid or liquid state.

Soon after the first successful nuclear magnetic resonance experiments,
was realized that the width of the observed resonance line for protons
as mostly due to inhomogeneities in the constant magnetic field used to
lit the energy sublevels. When a very homogeneous field was applied, the
oton resonance line was shown to exhibit a fine structure on the order of
01 G (10^{-6} T). This structure depends on the organic compound to which
e hydrogens of the sample belong. With even more homogeneous fields
hyperfine structure on the order of 0.001 G (10^{-7} T) is observed. It is
is fine structure that has made NMR such an important tool for analytical
emistry.

The term electron spin (or paramagnetic) resonance is used for tran-
ions between the Zeeman levels of quasi-free electrons in liquids and
lids. In principle, we should always measure a g factor of 2.00 (if we deal

with free electrons); instead a great variety of g factors and structure appears in the resonance lines due to the different effective coupling of the electron with the crystalline field. These effects depend on the relative orientation of the magnetic field B_0 and the crystal axis. Thus, electron spin resonance is a very important tool in the study of crystalline structures as well as in the identification of free radicals in chemistry, medicine, and biophysics.

This chapter is organized as follows. In Section 7.2 the conditions for inducing magnetic-dipole transitions are discussed from both the quantum and classical point of view. In Section 7.3 we introduce the mechanisms essential for the observation of energy absorption in nuclear magnetic resonance and electron spin resonance experiments, namely relaxation and saturation. We also discuss the idea of free induction decay and pulsed NMR. The techniques and results of nuclear magnetic resonance experiments with protons are presented in Section 7.4. We conclude with a discussion of an electron spin resonance experiment that operates at microwave frequencies.

As was the case in the previous chapter the discussion is limited, and the reader may wish to refer to some of the many excellent monographs and texts on this subject. A list of suggested references is given at the end of the chapter.

7.2. THE RATE FOR MAGNETIC-DIPOLE TRANSITIONS

7.2.1. Quantum Calculation

The experimental signals in NMR involve the participation of many nuclei. In this section, however, we will consider the effects associated with a single nucleus: we use the term *a single spin*. We will return to an ensemble of nuclei in Section 7.3.

Let us consider, for example, a nucleus with angular momentum $\mathbf{I}$ (magnitude $\hbar\sqrt{I(I+1)}$) and magnetic moment $\boldsymbol{\mu}$ oriented along the spin axis. For nuclei it is customary to express the proportionality between the spin $\mathbf{I}$ and magnetic moment $\boldsymbol{\mu}$ by

$$\boldsymbol{\mu} = \gamma \hbar \mathbf{I}, \tag{7.4}$$

where γ is called the gyromagnetic ratio; as can be seen from Eq. (7.6) below, γ has dimensions of radians per second–tesla. The gyromagnetic

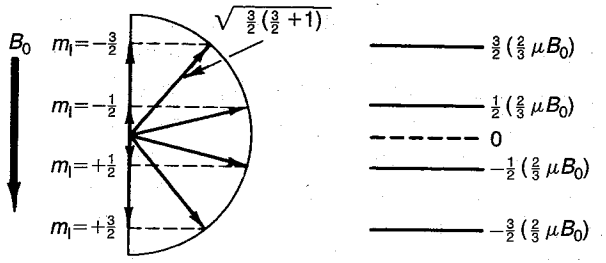

FIGURE 7.3 The energy of the four sublevels of a nucleus with spin $I = \frac{3}{2}$ when placed in a magnetic field B_0. Note that the energy depends on the "orientation" of the spin with respect to B_0; the magnitude of the spin vector is $|\mathbf{I}| = \sqrt{\frac{3}{2}(\frac{3}{2}+1)}$.

ratio γ cannot be calculated from a simple expression such as found for the g factor of atomic electrons in Eq. (6.17). (For instance, for the proton $\gamma = 5.586\ \mu_N$, where μ_N is the nuclear magneton.)

In the presence of an external magnetic field B_0, the nucleus can be in any of the $(2I + 1)$ sublevels labeled by m_I as shown also in Fig. 7.3. We can then write for the energy[2] of these sublevels (see Eq. (7.1))

$$\frac{E}{\hbar} = -\frac{1}{\hbar}\frac{\mu}{I} B_0 m = -\gamma B_0 m, \tag{7.5}$$

so that the energy difference between any adjacent sublevels ($\Delta m = \pm 1$) is simply

$$\frac{\Delta E}{\hbar} = \gamma B_0 = \omega_0. \tag{7.6}$$

Thus for protons in a field of 1 T the resonance frequency will be

$$\nu_0 = 5.586 \mu_N B_0 = 42.581\ \text{MHz} \qquad (B_0 = 1\ \text{T}).$$

Consider then the simplest case, namely, $I = \frac{1}{2}$, for which only two sublevels exist, $m = -\frac{1}{2}$ and $m = +\frac{1}{2}$. In addition to B_0, let a weak field H_1, rotating in a plane normal to B_0 with an angular frequency ω be introduced. Taking the z axis along B_0 we write the two components of H_1 as

$$(H_1)_x = H_x = H_1 \cos \omega t \qquad (H_1)_y = H_y = H_1 \sin \omega t,$$

[2]Instead of energy, we use for convenience angular frequency; the transition frequency is $\Delta\nu = (\Delta E/\hbar)/(2\pi) = \omega_0/2\pi$.

and we assume that

$$\mu_0 H_1 \ll B_0.$$

The additional energy of the nucleus, due to the field H_1, is

$$\mathcal{H}_1 = \boldsymbol{\mu} \cdot \mathbf{H}_1 = \gamma\hbar\left(H_x I_x + H_y I_y\right) = \frac{\gamma\hbar H_1}{2}\left(I_+ e^{-i\omega t} + I_- e^{+i\omega t}\right), \tag{7.7}$$

where[3]

$$I_+ = I_x + iI_y \qquad \text{and} \qquad I_- = I_x - iI_y. \tag{7.8}$$

Since the energy specified by Eq. (7.7) is very small as compared to that given by Eq. (7.5), it can be treated as a time-dependent perturbation[4]; thus, to first order, the transition probability is proportional to the absolute square of the matrix element

$$\mathcal{M} = \frac{\gamma\hbar H_1}{2}\langle f|I_+ e^{-i\omega t} + I_- e^{i\omega t}|i\rangle, \tag{7.9}$$

where i and f stand for the initial and final state. As usual the matrix element is evaluated by performing the integral

$$\mathcal{M} = \int \psi_f^* \mathcal{H}_1 \psi_i d^3x\, dt, \tag{7.10}$$

where $\mathcal{H}_1$ is the perturbing energy of Eq. (7.7). We must include the time dependence of the wave functions

$$\begin{aligned}\psi_f &= u(I, m') \exp\left(-i\tfrac{E'}{\hbar}t\right)\\ \psi_i &= u(I, m) \exp\left(-i\tfrac{E}{\hbar}t\right).\end{aligned} \tag{7.11}$$

Here primes refer to the final state, and $u(I, m)$ stands for the time-independent part of the wave function. Evaluating Eq. (7.9) with the help

[3]We expand the exponentials and obtain

$$\begin{aligned}&(I_x \cos\omega t + iI_y(-i)\sin\omega t) + (I_x \cos\omega t - iI_y(+i)\sin\omega t)\\ &\quad = 2(I_x \cos\omega t + I_y \sin\omega t).\end{aligned}$$

[4]See, for example, E. Fermi, *Notes on Quantum Mechanics*, Lecture 23, Univ. of Chicago Press, Chicago, 1961.

f Eqs. (7.10) and (7.11) we find that

$$\mathcal{M} = \frac{\gamma\hbar H_1}{2}\left\{\langle I, m'|I_+|I, m\rangle \int \exp\left[-i\left(\frac{E-E'}{\hbar}+\omega\right)t\right]dt \right.$$
$$\left. + \langle I, m'|I_-|I, m\rangle \int \exp\left[-i\left(\frac{E-E'}{\hbar}-\omega\right)t\right]dt\right\}. \tag{7.12}$$

The matrix elements of the operators I_+ and I_- are[5]

$$\langle m'|I_+|m\rangle = \sqrt{I(I+1)-m(m+1)}\,\delta_{m',m+1}$$
$$\langle m'|I_-|m\rangle = \sqrt{I(I+1)-m(m-1)}\,\delta_{m',m-1},$$

nd thus I_+ connects only states with $m' - m = 1$ while I_- connects ates $m' - m = -1$. For $I = \frac{1}{2}$ the above matrix elements reduce to 1 or either I_+ or I_-. The integrals over time in Eq. (7.12) are essentially functions (but see below) expressing the conservation of energy and nowing that the transition probability is different from zero only if

$$E' - E = \hbar\omega \qquad \text{for } m' = m+1$$

nd

$$E - E' = \hbar\omega \qquad \text{for } m' = m-1, \tag{7.13}$$

at is, when the angular frequency of the rotating field is equal to the energy fference between adjacent m sublevels. Using Eq. (7.6), the conditions f Eqs. (7.13) become simply

$$\hbar\omega = \hbar\gamma B_0 = \hbar\omega_0.$$

To complete the calculation of the transition rate we must integrate (the bsolute square of Eq. (7.12)) over the density of final states. This leads to ermi's golden rule[6]

$$R_{if} = \frac{2\pi}{\hbar}|\mathcal{M}|^2\rho(E), \tag{7.14}$$

[5] See E. Fermi (1961), Lecture 28.

[6] See E. Fermi (1961), or L. Shiff, *Quantum Mechanics*, Chapter 8, McGraw-Hill, ew York, 1968.

where R_{if} is the *transition probability per unit time* (or transition rate) from the initial state i to the final state f. In Eq. (7.14), $\mathcal{M}$ is the time-independent part of the matrix element given by Eq. (7.12) (that is, without the integrals). $\rho(E)$ is the "density of final states" and gives the number of states f per unit energy interval that have energy close to E'. For example, if the final state f has an extremely well-defined energy E_0, then $\rho(E) \to \delta(E - E_0)$; if the final state has a certain width due for instance to a finite lifetime or other broadening effects, then $\rho(E)$ expresses this fact mathematically. We require the function $\rho(E)$ to be normalized and can also express it in terms of frequency

$$\rho(E) = \rho(h\nu) = \frac{1}{h}\,g(\nu)$$

with

$$\int \rho(E)\,dE = \int g(\nu)\,d\nu = 1. \tag{7.15}$$

Combining Eqs. (7.12), (7.14), and (7.15) we obtain for the transition rate in the case $I = \frac{1}{2}$ the elegant result

$$R_{-1/2\to+1/2} = R_{+1/2\to-1/2} = \frac{\gamma^2 H_1^2}{4}\,g(\nu). \tag{7.16}$$

In the above equation ν is the frequency of the perturbing field (RF or microwave), and $g(\nu)$ gives the shape of the resonance line; note that $g(\nu)$ will be significantly different from zero only for $\nu \approx \nu_0$. Note also that in Eq. (7.16) and in the equations leading up to it, H_1 must be expressed in tesla, namely its value in amperes per meter must be multiplied by the permeability of free space μ_0. We have deliberately not included this factor in the equations to avoid confusion with the symbol for magnetic moments.

There are two important comments we want to make at this point. First as can be seen from Eq. (7.12) or (7.16) the rotating field H_1 will induce transitions from $m_i = -\frac{1}{2}$ to $m_f = +\frac{1}{2}$ with exactly the same probability as from $m_f = +\frac{1}{2}$ to $m_i = -\frac{1}{2}$. As a result, in the presence of the field H_1 both levels will, on average, be *equally populated*. This argument remains valid for any value of the nuclear spin. Secondly, while we used a perturbative calculation the two-level system can be solved exactly in terms of simple functions as described, for instance, in the *Feynman Lectures*,

Vol. III, Lecture 30.[7] We will make use of the exact solution in Section 7.3.4 when we discuss pulsed NMR and free induction decay.

7.2.2. Classical Interpretation

Below we show how the effect of a rotating radiofrequency field can be understood also on the basis of a classical model. Consider again a nucleus with spin **I** and magnetic moment $\boldsymbol{\mu} = \gamma\hbar\mathbf{I}$. Let J be the magnitude of the angular momentum, which classically[8] will be just $J = \hbar I$, and let it make an angle θ with the z axis as shown in Fig. 7.4a. If a constant magnetic field B_0 is applied along the z axis, the field will exert a torque on the magnetic moment, given by

$$\boldsymbol{\tau} = \boldsymbol{\mu} \times \boldsymbol{B_0} = \gamma(\boldsymbol{J} \times \boldsymbol{B_0}). \tag{7.17}$$

This must equal the time derivative of the angular momentum

$$\frac{d\mathbf{J}}{dt} = \boldsymbol{\tau} = \gamma(\boldsymbol{J} \times \boldsymbol{B_0}). \tag{7.18}$$

The solution of Eq. (7.18) leads to a precession of the angular momentum vector **J** about the z axis, preserving the angle θ, and at an angular frequency ω_0 independent of θ,

$$\boldsymbol{\omega_0} = -\frac{|d\mathbf{J}/dt|}{|\boldsymbol{J} \times \boldsymbol{n}_z|}\,\mathbf{n}_z = -\gamma B_0 \mathbf{n}_z, \tag{7.19}$$

where $\mathbf{n}_z$ is the unit vector in the z direction.

This phenomenon is called the *Larmor precession* and the angular frequency given by Eq. (7.19) is the "Larmor" frequency. It is fascinating even though not surprising that the Larmor frequency has the same value as given by Eq. (7.6) for the transition frequency between any adjacent levels ($\Delta m = \pm 1$). Further, since the angle θ is preserved, the energy of the nucleus in the magnetic field remains a constant

$$E = -\boldsymbol{\mu} \cdot \boldsymbol{B_0} = -\gamma\hbar I B_0 \cos\theta. \tag{7.20}$$

We now introduce an additional weak magnetic field $\mathbf{H}_1$ oriented in the x–y plane and rotating about the z axis (in the same direction as the

[7] See also A. Das and A. C. Melissinos, *Quantum Mechanics*, Section 5.1, Gordon and Breach, New York, 1986.

[8] Instead of its quantum-mechanical (QM) value $I = \hbar\sqrt{I(I+1)}$.

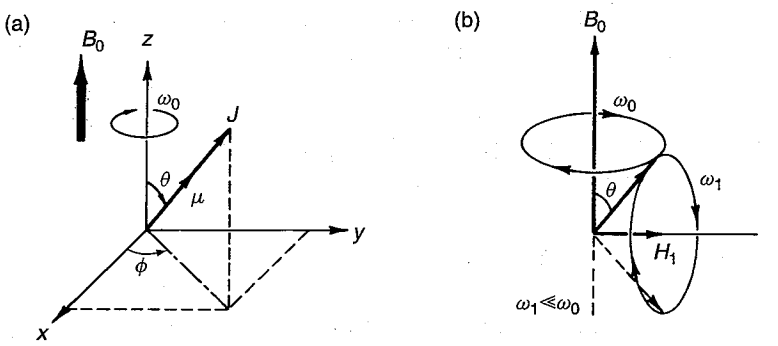

FIGURE 7.4 Precession of a magnetic moment μ when placed in a magnetic field B_0. (a) The spin precesses with angular frequency $\omega_0 = \gamma B_0$; the angle θ is a constant of the motion. (b) In addition to B_0 a weak magnetic field H_1 is now also applied. H_1 is rotating about the z axis with angular frequency ω_0 and therefore μ precesses about $\mathbf{H}_1$ with angular frequency $\omega_1 = \gamma H_1$; θ is no longer conserved.

"Larmor precessing" spin **I**) with an angular frequency ω. If the frequency ω is different from ω_0, the angle between the field $\mathbf{H}_1$ and the magnetic moment μ will continuously change so that their interaction will average out to 0. If, however, $\omega \approx \omega_0$, the angle between μ and $\mathbf{H}_1$ is maintained and a net interaction is effective (Fig. 7.4b). If we look at the system in a reference frame *rotating about the z axis with the angular velocity* ω_0, then the spin will appear to make an angle $\psi = 90° - \theta$ with H_1 and according to the previous argument will start to precess (in the rotating frame) about H_1. This corresponds to a "nutation" and a consequent change of the angle θ, which implies a change in the potential energy of the nucleus in the magnetic field (Eq. (7.20)). The change in θ is the classical analogy to a *transition* between sublevels with different m. We see that (a) such transitions may take place only if the rotating field has an angular frequency $\omega = \omega_0 = \gamma B_0$, and (b) that the angle θ will continuously change with an angular frequency $\omega_1 = \gamma H_1$. The effect of the radiofrequency is to populate, on the average, all values of θ, that is, *all levels, equally.*

However, if the field H_1 is applied only for a short time t, such that $\omega_1 t = \pi$, then a spin that was originally at an angle θ (w.r.t the z axis) will find itself at an angle $\pi - \theta$ (or at an angle θ from the $-z$ axis). This is the equivalent of the QM transition from $m = -\frac{1}{2}$ to $m = +\frac{1}{2}$. If the field is applied for a time t such that $\omega_1 t = 2\pi$, then the spin will end up at the same angle w.r.t the z axis (in the same state) and so on. By applying

RF pulses of selected duration we can thus manipulate the spin state. We will make use of this idea in Section 7.3.4.

7.3. ABSORPTION OF ENERGY BY THE NUCLEAR MOMENTS

7.3.1. Relaxation and Saturation

We saw in the previous section that a radiofrequency magnetic field may induce transitions between the magnetic sublevels of a nucleus, electron, or atom. In the case of atomic-beam experiments the atoms are free, while in nuclear magnetic resonance or electron spin resonance experiments the nuclei or electrons are in constant interaction with their surroundings. There are mainly two types of interactions: (a) *spin–lattice*, by which we mean the interaction with the thermal bath that tends to restore the Boltzmann distribution, where the spin can relax by transferring energy to the lattice; and (b) *spin–spin*, in which the nuclear spin interacts with a neighboring nuclear spin, but the total energy of the spin system remains constant. As a matter of fact, it is the spin–lattice interaction that makes possible the observation of energy absorption from the radiofrequency field when the resonance frequency is reached.

To understand this last statement, consider again the simple case of a nucleus with spin $I = \frac{1}{2}$. In the presence of a magnetic field B_0 it is split into the two energy sublevels with $m = +\frac{1}{2}$ and $m = -\frac{1}{2}$. As remarked before, the rate (Eq. (7.16)) for transitions

$$\left(m = +\frac{1}{2}\right) \rightarrow \left(m = -\frac{1}{2}\right) \tag{7.21a}$$

equal to the rate for transitions

$$\left(m = -\frac{1}{2}\right) \rightarrow \left(m = +\frac{1}{2}\right). \tag{7.21b}$$

The number of transitions per unit time is given in either case by

$$R_{if} \times N_i, \tag{7.22}$$

where N_i is the number of nuclei in the initial state. Further, transitions of the type in Eq. (7.21a) absorb energy from the radiofrequency field, whereas

transitions of the type in Eq. (7.21b) give energy to the radiofrequency field (recall Eq. (7.5)). Thus the net power absorbed from the radiofrequency field is (we also multiply by the energy necessary for one transition)

$$\begin{aligned} P &= \left[N_{+1/2} \times R\left(+\frac{1}{2} \rightarrow -\frac{1}{2}\right)\right]\hbar\omega_0 \\ &\quad - \left[N_{-1/2} \times R\left(-\frac{1}{2} \rightarrow +\frac{1}{2}\right)\right]\hbar\omega_0 \\ &= \left(N_{+1/2} - N_{-1/2}\right) R\hbar\omega_0. \end{aligned} \tag{7.23}$$

Thus if $N_{-1/2} = N_{+1/2}$, no net power can be absorbed from the field. However, if we consider a system consisting of a large number of spins in equilibrium with its surroundings, it is known from a very general theorem of statistical mechanics that every state of energy E will be populated according to the Boltzmann distribution

$$N(E) = N_0 e^{-E/kT} \tag{7.24}$$

with k the Boltzmann constant and T the absolute temperature in Kelvins. It follows that for a system of N particles with spins I in the presence of a magnetic field B_0, each m sublevel will be populated according to

$$N(m) = \frac{N}{2I+1} \exp\left(+\frac{m\gamma\hbar B_0}{kT}\right). \tag{7.25}$$

The normalizing factor was approximated by $N/(2I+1)$, which holds[9] for $\gamma\hbar B_0 \ll kT$; $-m\gamma\hbar B_0$ is the energy of the m sublevel. Note that T in Eq. (7.25) is the temperature of the spin system and equals the lattice temperature, if no external perturbations (such as the radiofrequency field) are present.

It follows from Eq. (7.25) that the populations $N_{+1/2}$ and $N_{-1/2}$ entering Eq. (7.23) of our previous discussion ($I = \frac{1}{2}$) will not be equal. There will be a number of excess nuclei N_s, in the lower energy state given by

$$N_s = N_{+1/2} - N_{-1/2} = \frac{N}{2}\left[\exp\left(+\frac{\hbar\omega_0}{2kT}\right) - \exp\left(-\frac{\hbar\omega_0}{2kT}\right)\right],$$

[9] Expand the exponential through first order, to obtain correctly

$$\sum_{m=-I}^{m=+I} N(m) = N.$$

since $\hbar\omega_0$ is always much smaller than kT, we may write for the above ation

$$N_s \approx \frac{N}{2}\frac{\hbar\omega_0}{kT}. \tag{7.26}$$

only these N_s nuclei that can contribute toward a net absorption of rgy, and the power absorbed from the RF field is given by

$$P = N_s \times R \times \hbar\omega_0 = \frac{N}{2}\frac{(\hbar\omega_0)}{kT} \times (\hbar\omega_0) \times R. \tag{7.27}$$

Before proceeding further, we introduce some numerical values: for ons $\gamma = 2.673 \times 10^8$ rad/s-T, so that for $B_0 = 1$ T and $T = 300$ K we ain

$$\frac{N_s}{N} = \frac{\omega_0\hbar}{2kT} = \frac{(2.67 \times 10^8) \times (6.6 \times 10^{-16})\ \text{eV}}{2(1/40)\ \text{eV}} \approx 4 \times 10^{-6},$$

ch justifies the approximation used to obtain Eq. (7.26). If we further sider a sample of 1 cm^3 of water, the number of protons contained in

$$N = N_0 \times (2/18) = 6 \times 10^{23} \times (2/18) = (2/3) \times 10^{23}.$$

e use for $R = 1$/s (as can be seen from Eq. (7.16), this is a conservative ue; R, however, can be as large as 10^3/s as discussed below), we obtain n Eq. (7.27)

$$P = (\hbar\omega_0) \times \left(N \times \frac{\hbar\omega_0}{2kT_s}\right) \times R \simeq 5 \times 10^{10}\ \text{eV/s} = 8 \times 10^{-9}\ \text{W}. \tag{7.28}$$

s is a very small amount of power, especially since the applied radiofre- ncy field may be on the order of milliwatts. Therefore, a sensitive null hod greatly facilitates the observation of nuclear resonance absorption. n writing Eq. (7.27), we assumed that the power absorbed is propor- al to the number of excess nuclei which we now designate by n_s; vever, as transitions are induced to the upper state, the number n_s will tinuously decrease. The decrease will be exponential at the rate R

$$n_s = N_s e^{-Rt}.$$

n the populations of the two levels will be practically equalized, $_{1/2} \simeq N_{-1/2}$, and no more absorption will be observed.

However, while the radiofrequency field tends to equalize the populations, the "spin–lattice" interaction tends to restore the Boltzmann distribution at a rate characterized by $1/T_1$. We say that the nuclei are "relaxing" through their interaction with the lattice, and the characteristic time T_1 for this process is called the *spin–lattice relaxation time*. Therefore, in the presence of a radiofrequency field tuned to the resonance frequency, the number of excess nuclei at equilibrium n_s depends on T_1 and on R; if $R \ll 1/T_1$, then $n_s \to N_s$, while if $R \gg 1/T_1$, $n_s \to 0$. The value of n_s can be easily obtained[10]

$$n_s = \frac{N_s}{1 + 2RT_1}, \tag{7.29}$$

where N_s (Eq. (7.27)) is the equilibrium excess of population in the absence of the radiofrequency field.

By using Eq. (7.16) for R, we obtain

$$n_s = \frac{N_s}{1 + \frac{1}{2}\gamma^2 H_1^2 T_1 g(\nu)}. \tag{7.30}$$

From the above result we see that when too much radiofrequency power is used, the number of excess nuclei n_s decreases, and so does the resonance signal. We say that the sample has been saturated, and the ratio n_s/N_s is frequently referred to as the saturation factor Z:

$$\frac{n_s}{N_s} = \frac{1}{1 + \frac{1}{2}\gamma^2 H_1^2 T_1 g(\nu)} \equiv Z. \tag{7.31}$$

---

[10] Let $n = n_{+1/2} - n_{-1/2}$ be the instantaneous excess of nuclei in the presence of both radiofrequency and relaxation. The effect of the radiofrequency is to make $n \to 0$

$$\left(\frac{dn}{dt}\right)_{\text{RF}} = -2Rn.$$

(The factor of 2 arises because each transition up decreases $n_{+1/2}$ by 1, and also increases $n_{-1/2}$ by 1.) The effect of relaxation is to return $n \to N_s$

$$\frac{d(N_s - n)}{dt} = -(N_s - n)\frac{1}{T_1} = -\left(\frac{dn}{dt}\right)_{\text{relax}}.$$

Equilibrium is reached when the sum of the two rates is zero; that is,

$$-2Rn + \frac{N_s - n}{T_1} = 0$$

which yields Eq. (7.29).

The maximum useful value of the radiofrequency power therefore depends on the relaxation time T_1. For solids, T_1 is large (it takes a long time for the spins to reorient themselves in the equilibrium position), and therefore only weak radiofrequency fields may be applied. For example, for protons in ice $T_1 = 10^4$ s. In contrast, in liquids, especially in solutions containing paramagnetic ions, the relaxation time for protons may be as short as $T_1 = 10^{-4}$ s.

7.3.2. Line Width and T_2

Just as optical spectral lines can be broadened by external factors (see Section 6.4) the NMR signal is not perfectly sharp but has a certain width. Excluding inhomogeneities of the magnetic field B_0 over the size of the sample, the principal cause for the line width is the interaction between neighboring spins. In the classical analogy of Section 7.2.2 we say that the spin–spin interaction is destroying the phase coherence between the precessing spins and the rotating radiofrequency field. Another way of thinking of the spin–spin interaction is that one nuclear spin produces a local magnetic field B_{local} at the position of another spin, which then finds itself in a field

$$B_0' = B_0 + B_{\text{local}}$$

and consequently has a resonance frequency $\omega_0' = \gamma B_0'$ slightly different from ω_0. To estimate this effect, we calculate the magnetic field produced by a magnetic dipole one nuclear magneton strong, at a typical distance of 0.1 nm.

$$B_{\text{local}} \approx \left(\frac{\mu_0}{4\pi}\right)\frac{\mu_N}{r^3} = \left(\frac{\mu_0}{4\pi}\right) \times \frac{e\hbar}{2M_p} \times \frac{1}{r^3},$$

where μ_N is the nuclear magneton $e\hbar/2M_p$ and $\mu_0 = 4\pi \times 10^{-7}$ V-s/A-m is the permeability of free space. Numerically we find that

$$B_{\text{local}} \simeq 5 \times 10^{-4} \text{ T},$$

which is a significant broadening of the line. In liquids and gases, however, the reorientation of the molecules is so fast that the average local field is very close to zero, and therefore very narrow lines can be obtained.

In Eqs. (7.15) and (7.16) we introduced the function $g(\nu)$ to describe the width of the NMR line. We now see that this width is mainly due to

the spin–spin interaction. Since $g(\nu)$ has dimensions of inverse frequency, namely, of time, we *define* one-half of its maximum value by T_2

$$\frac{1}{2}\, g(\nu_0) = T_2, \tag{7.32}$$

where ν_0 is the resonance frequency in the absence of any broadening effects. T_2 is called the *transverse relaxation time*. In view of the normalization condition (Eq. (7.15)),

$$\int g(\nu)\, d\nu = 1,$$

(which also fixes the dimensions of $g(\nu)$), we see that a short T_2 implies broad lines, whereas when T_2 is long, the line is narrow.

Using the definition of Eq. (7.32), we can then write for the saturation factor Z (Eq. (7.31)) at resonance

$$Z_0 = Z(\nu_0) = \frac{1}{\left[1 + \gamma^2 H_1^2 T_1 T_2\right]}. \tag{7.33}$$

It is of interest to estimate T_2 for protons when $B_{\text{local}} = 5 \times 10^{-4}$ T as found previously. From the uncertainty principle $\Delta E \Delta t \sim \hbar$ and the line width $\Delta E = \gamma B_{\text{local}}$ so that

$$T_2 \sim \Delta t \sim \frac{1}{B_{\text{local}}}\,\frac{1}{(5.58\mu_N/\hbar)} \sim 7 \times 10^{-6} \text{ s},$$

where we used $\gamma_p = 5.58$ and $\mu_N/\hbar = 2\pi \times 7.62$ MHz/T (see Eq. (7.2)).

Finally, as already mentioned, inhomogeneities in the magnetic field introduce spurious broadening effects that not only mask the fine structure of the line but also decrease the signal amplitude: hence the use of very homogeneous magnets and of the "spinning sample" technique.

7.3.3. The Bloch Magnetic Susceptibilities[11]

F. Bloch, who shared with E. M. Purcell the Nobel prize for the discovery of NMR, gave a macroscopic description of nuclear magnetic resonance,

[11] This section may be omitted without a loss of continuity and the reader can proceed directly to the discussion of the experimental technique and results in Section 7.4. However, the discussion should be quite helpful for understanding the meaning of the "dispersion" curve as well as the observed line shapes for both absorption and dispersion.

here the effect of the RF field is accounted for by the *polarization* of the clear spins. We know that when an electric (or magnetizing) field E (or) is applied in a region containing matter, the material becomes polarized r magnetized). We write

$$\mathbf{P} = \chi_e \mathbf{E} \qquad \mathbf{M} = \chi_\mu \mathbf{H}, \tag{7.34}$$

here χ_e and χ_μ are the electric and magnetic susceptibilities. The polarizaon is due primarily to the alignment of the permanent electric (magnetic) pole moments of the atoms or molecules in the direction of the applied ld. Materials that have such dipole moments and exhibit large polaration should be called *paraelectric* (or for large magnetization, they are deed called *paramagnetic*).

The refractive index of light is related to the electric and magnetic sceptibilities, since

$$\epsilon = (1 + \chi_e)\epsilon_0 \qquad \mu = (1 + \chi_\mu)\mu_0$$

nd

$$n = \frac{c}{c'} = \frac{1/(\sqrt{\epsilon_0 \mu_0})}{1/(\sqrt{\epsilon \mu})} = \sqrt{(1 + \chi_e)(1 + \chi_\mu)}.$$

he refractive index and therefore also the susceptibilities are a function of e frequency, as is evident from the familiar phenomenon of the dispersion f light. Thus the susceptibility at optical frequencies differs from the static ne and is a function of the frequency.[12] Frequently the transmission of ght through matter is accompanied by absorption that may be strongest a particular resonant frequency. We may account for the absorption by ttributing an imaginary part to the susceptibility.

The same formalism can be used as well for the description of nuclear agnetic resonance phenomena. The static susceptibility arising from e *nuclear* moments in an otherwise diamagnetic material differs from ero, but is very small and difficult to measure. For the radiofrequency usceptibility, we write

$$\chi(\omega) = \chi'(\omega) - i\chi''(\omega),$$

[12]For optical frequencies and for almost all materials, χ_μ is 0 and the variation in n arises ntirely from χ_e.

where both $\chi'(\omega)$ and $\chi''(\omega)$ exhibit a resonant behavior when ω reaches $\omega_0 = \gamma B_0$. The real part $\chi'(\omega)$ is given by

$$\chi'(\omega) = \frac{1}{2}\chi_0 \omega_0 T_2 \left[\frac{(\omega_0 - \omega)T_2}{1 + (\omega_0 - \omega)^2 T_2^2 + \gamma^2 H_1^2 T_1 T_2}\right], \tag{7.35}$$

while the imaginary part $\chi''(\omega)$ is given by

$$\chi''(\omega) = \frac{1}{2}\chi_0 \omega_0 T_2 \left[\frac{1}{1 + (\omega_0 - \omega)^2 T_2^2 + \gamma^2 H_1^2 T_1 T_2}\right]. \tag{7.36}$$

Here χ_0 is the static magnetic susceptibility defined as in Eq. (7.34)

$$M_0 = \chi_0 H_0,$$

and T_1 and T_2 are the familiar relaxation times introduced before; the term $\gamma^2 H_1^2 T_1 T_2$ appearing in the denominator is a measure of the saturation as defined in Eq. (7.31).

Equations (7.35) and (7.36) are shown in Fig. 7.5 under the assumption that $\gamma^2 H_1^2 T_1 T_2 \ll 1$; they have the typical behavior of a dispersion and a power resonance curve. We also note that Eq. (7.35) is proportional to the derivative, with respect to ω, of Eq. (7.36). By adjusting the detection equipment, we may observe experimentally either of those curves, or a combination of both, as a function of $\omega_0 - \omega$. Experimentally we can vary

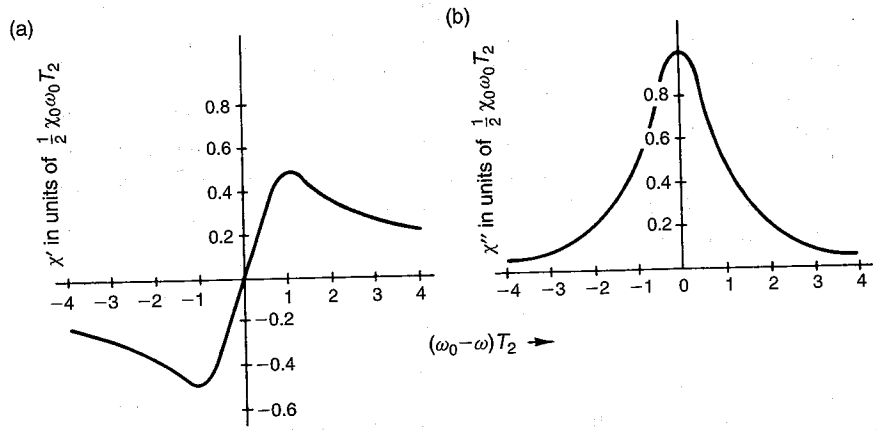

FIGURE 7.5 The radiofrequency magnetic susceptibilities near resonance. (a) The real part of the susceptibility exhibits a typical dispersion shape (Eq. (7.35)). (b) The imaginary part of the susceptibility exhibits a typical absorption shape (Eq. (7.36)).

$\omega_0 - \omega$ either by sweeping the magnetic field (changes $\omega_0 = \gamma B_0$) at fixed RF frequency, or by sweeping the RF frequency ω, while keeping the field B_0 fixed.

7.3.4. Free Induction Decay and Pulsed NMR[13]

It is convenient to consider again the classical interpretation of NMR discussed in Section 7.2.2. Refer to Fig. 7.4b and assume that the RF field is applied along the x' axis in the rotating frame, for a short time t, such that $\omega_1 t = \gamma H_1 t = \pi/2$. Then the net magnetization vector **M** will be rotated into the x'–y' plane; in fact it will be along the y' axis. In the laboratory frame this situation corresponds to a magnetization vector rotating in the x–y plane with angular frequency $\omega_0 = \gamma B_0$ around the z axis. A coil is fixed in the laboratory frame with its axis in the x–y plane. Then the rotating magnetization will *induce* an RF signal in the coil at frequency ω_0. Recall that now $\mathrm{M}(t) = \mathrm{M}_x \cos \omega t + M_y \sin \omega t$. This sequence is shown in Figs. 7.6a and 7.6b.

How long will the signal persist after time t? First of all because the spins are in contact with the lattice there will be a tendency for **M** to return into alignment with the z axis (recall that there is no RF field after time t). This relaxation process is characterized by the time T_1, the spin–lattice relaxation time introduced in Eq. (7.29). Usually, however, T_1 is fairly long and the individual spins that contribute to **M** become *dephased* either because of field inhomogeneities or because of the spin–spin interaction. When the spins are completely dephased (i.e., when they are pointing uniformly in all directions in the x–y plane) $d\mathbf{M}/dt$ through the coil vanishes and so does the induced signal. This effect occurs on a time scale T_2, which is usually shorter than T_1. Thus we observe a decaying exponential as shown in Fig. 7.6c. In general the decay constant is designated by T_2^* and contains the effects of the spin–spin interaction, magnetic field inhomogeneity, and spin–lattice relaxation

$$\frac{1}{T_2^*} = \frac{1}{T_2} + \frac{1}{T_1} + \gamma \Delta B_0. \tag{7.37}$$

[13]This section, too, can be omitted on a first reading without loss of continuity. However, it provides insight on the interpretation of transient effects and of the modern NMR techniques that are based on pulsed excitation rather than continuous wave (CW) measurements.

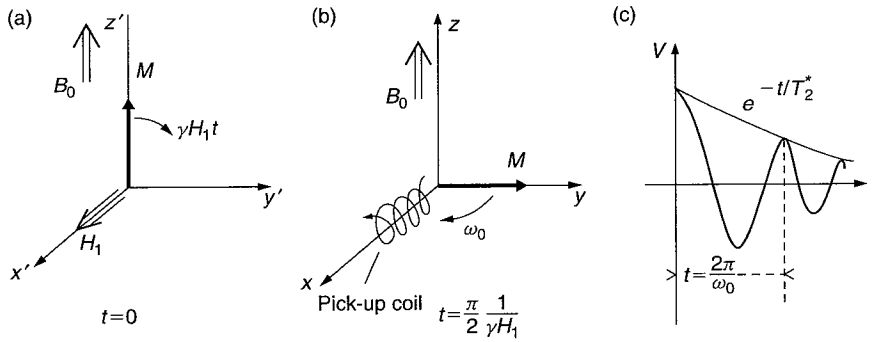

FIGURE 7.6 Free induction decay following a $\pi/2$ RF pulse. (a) The magnetization vector M in the rotating frame of reference before the application of the RF ($t = 0$). (b) After the $\pi/2$ pulse, the M vector will precess in the stationary frame with angular velocity ω_0. (c) The induced signal in a stationary coil in the x–y plane will have period $T = 2\pi/\omega_0$ and will decay exponentially with time constant T_2^*.

Therefore the free induction decay (FID) signal contains information on both the resonant frequency ω_0 (namely on γ) and on T_2 for the sample being investigated.

Note that if one performs a Fourier transform on the FID signal, which is acquired in the time domain, we obtain the spectrum of *all* the resonant frequencies of the sample. This is much more convenient and efficient than searching for each resonant line separately.

We now briefly return to the quantum-mechanical description of these phenomena. It was mentioned in Section 7.2.1 that the response of a two-level system to a resonant perturbation can be solved *exactly* in quantum mechanics.[14] If at $t = 0$ the spin is in state $m = -\frac{1}{2}$ the probability of finding it at time t in state $m = +\frac{1}{2}$ is

$$P_{+1/2} = \sin^2(\omega_1 t/2), \tag{7.38a}$$

with $\omega_1 = \gamma H_1$. The probability for the spin to remain in state $m = -\frac{1}{2}$ is

$$P_{-1/2} = \cos^2(\omega_1 t/2), \tag{7.38b}$$

as it must be since for a two-level system it must hold that $P_{-1/2} + P_{+1/2} = 1$.

[14]See footnote 7 of this chapter.

First we reconcile the result of Eq. (7.38a) with our perturbative calcu-
tion for the transition rate obtained in Eq. (7.16). The transition rate is,
course, the time derivative of the probability and we have

$$\frac{dP_{-1/2\to+1/2}}{dt} = \frac{\omega_1}{2}\sin\omega_1 t = \frac{\gamma H_1}{2}\sin\omega_1 t.$$

ne perturbative calculation is valid when $\omega_1 t \ll 1$, and therefore we can
pand $\sin\omega_1 t$ to first order to find that

$$\frac{dP_{-1/2\to+1/2}}{dt} = \frac{\gamma^2 H_1^2}{2}\, t. \tag{7.39}$$

his result seems different from Eq. (7.16) but we realize that Eqs. (7.38)
e valid as long as the initial and final states are not otherwise disturbed
er the time interval t. The maximum such time is given by $T_2 = \frac{1}{2}\, g(\nu_0)$
ee Eq. (7.32)). Thus

$$\frac{dP_{-1/2\to+1/2}}{dt} = \frac{\gamma^2 H_1^2}{4}\, g(\nu_0)$$

expected from Eq. (7.16); we recall that in deriving Eqs. (7.38) it was
sumed that $\omega = \omega_0$. Note also that

$$\left|\frac{dP_{+1/2\to-1/2}}{dt}\right| = \left|\frac{dP_{-1/2\to+1/2}}{dt}\right|$$

repeatedly emphasized for the transition rate.
It is clear that applying a π-pulse ($\omega_1 t = \pi$) to a spin $\frac{1}{2}$ in the state
$= -\frac{1}{2}$ will make $P_{+1/2} = 1$ and $P_{-1/2} = 0$; namely the spin will flip
ites, as we also concluded from the classical analogy in Section 7.2.2.
owever, what is the result of a $\pi/2$-pulse ($\omega_1 t = \pi/2$)? Then we find
at

$$P_{+1/2} = \frac{1}{2} = P_{-1/2}.$$

mely the spin is in a coherent superposition of the $m = +\frac{1}{2}$ and $m = -\frac{1}{2}$
tes. It is described by a wave function

$$\psi = \frac{1}{\sqrt{2}}\left[\left|m_z = +\frac{1}{2}\right\rangle + \left|m_z = -\frac{1}{2}\right\rangle\right]. \tag{7.40}$$

This represents a spin oriented in the x–y plane, and in the presence of a magnetic field B_0 along the z axis it will precess[15] in this plane with angular frequency $\omega_0 = \gamma B_0$. The quantum and classical descriptions lead to precisely the same conclusions.

We conclude with the remark that the same formalism is used for atoms when two states of energy E_1 and E_2 are connected by an electric-dipole moment d. If such an atom is subject to an oscillatory electric field $\mathcal{E}_1$ at the resonant frequency between the states, $\omega_0 = (E_f - E_i)/\hbar$, transitions will occur. Of course ω_0 is now an optical frequency rather than RF frequency. If the atom is initially in the state $|i\rangle$ and the optical field is switched on at $t = 0$, the probability[16] for finding the atom in the state $|f\rangle$ at time t is

$$P_f(t) = \sin^2\left(\frac{\mathcal{E}_1 d}{2\hbar}\, t\right), \tag{7.41a}$$

and for finding it in the state $|i\rangle$

$$P_i(t) = \cos^2\left(\frac{\mathcal{E}_1 d}{2\hbar}\, t\right). \tag{7.41b}$$

These are of course the exact analogues to Eq. (7.38).

The precession frequency for the atomic case $\Omega_1 = \mathcal{E}_1 d/2\hbar$ is called the Rabi frequency. With the availability of lasers one can achieve strong enough electric fields to generate $\pi/2$, π, etc., optical pulses. In this way atoms can be placed in specific quantum states. Such manipulation of single atoms has recently found applications in quantum cryptography, and it could eventually lead to quantum computing.

7.4. EXPERIMENTAL OBSERVATION OF THE NUCLEAR MAGNETIC RESONANCE OF PROTONS

7.4.1. General Considerations

To observe nuclear magnetic resonance we need a sample, a magnet, a source of electromagnetic radiation of the appropriate frequency, and a detection system.

[15] See Das and Melissinos (1986) cited in Footnote 7 of this chapter.

[16] Here we gloss over the fact that d is really the matrix element of the electric-dipole operator between the initial and final states.

The magnetic field should be fairly homogeneous, and therefore it is advisable to choose a good magnet with polefaces at least 4 to 6 in. in diameter. As discussed in Section 7.3.2 inhomogeneities in the magnetic field broaden the line and reduce the peak amplitude; to obtain reasonable results, the inhomogeneities over the volume of the sample should be less than 1/1000. The choice of the field strength is arbitrary, provided the resulting frequency lies in a convenient radiofrequency band. However, since the signal-to-noise ratio increases (improves) as $\nu_0^{3/2}$, high fields are preferable; commonly, magnetic fields of 0.5 to 1 T are used, and for protons this corresponds to frequencies of 20 to 40 MHz.

The sample can be any material containing an ample supply of protons: paraffin, water, mineral oil, or any organic substance containing hydrogens will, in general, give a proton nuclear magnetic resonance signal. Some care must be exercised to avoid materials with long spin–lattice relaxation times T_1, since they will saturate at very low levels of radiofrequency power and therefore give weak signals (see Eq. (7.33)). Similarly it is profitable to have a narrow line; hence materials with long spin–spin relaxation time T_2 are chosen. Liquids will meet this condition, and in most instances the width of the line will be determined by the magnet inhomogeneity ($T_2 = 3 \times 10^{-4}$ s will give for protons a line width of 10^{-5} T). Plain tap water makes a good sample, or tap water doped with 1 wt% manganese nitrate $Mn(NO_3)_2$ or copper sulfate.

The size of the sample is limited by the area over which the magnet is homogeneous, but also by practical considerations of the coil used to couple the radiofrequency to the sample. In usual practice a 1-cm^3 sample is adequate; it is contained in a small tubular glass container, around which is wrapped a radiofrequency coil as shown in Fig. 7.7a. The whole assembly is then inserted into the magnet gap and should be secured firmly, since vibration is picked up by the coil and appears as noise in the detector.

In deriving the probability for a transition between the m sublevels, and in all our previous discussion, we have assumed the existence of a *rotating* field at the angular frequency ω close to ω_0. In practice, a magnetic field oscillating linearly as $A \sin \omega t$ is established in the interior of the radiofrequency coil (Fig. 7.7a). Linear harmonic motion, however, is equivalent to two rotations in opposite direction of amplitude $A/2$ as shown in Fig. 7.7b since

$$A \cos \omega t \mathbf{n}_x = \frac{A}{2}(\cos \omega t \mathbf{n}_x + \sin \omega t \mathbf{n}_y) + \frac{A}{2}(\cos(-\omega t)\mathbf{n}_x + \sin(-\omega t)\mathbf{n}_y), \tag{7.42}$$

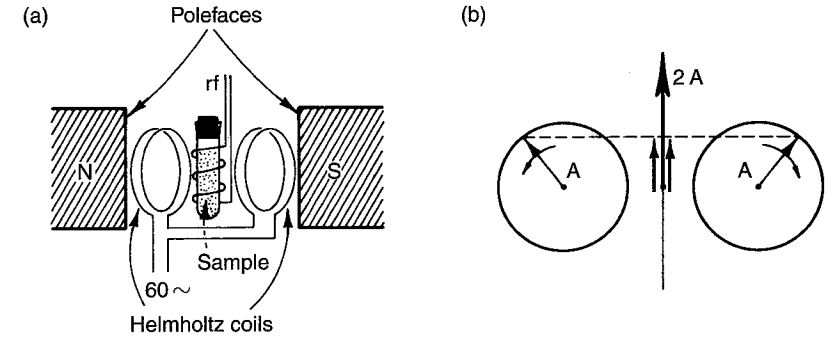

FIGURE 7.7 (a) Schematic arrangement of a nuclear magnetic resonance apparatus. The sample is placed in a homogeneous magnetic field and radiofrequency is coupled to it by means of the coil. The Helmholtz coils are used to modulate the constant magnetic field. (b) A linearly oscillating field of frequency ω is equivalent to two fields rotating in opposite directions with the same frequency ω.

where $\mathbf{n}_x$ and $\mathbf{n}_y$ are unit vectors in the x and y directions. The component rotating in the same direction as the precessing spins will be in resonance and may cause transitions; the other component is completely out of phase and has no effect on the sample.

When the radiofrequency reaches the resonance value ω_0, energy is absorbed from the field in the coil and this fact is sensed by the detector. Because of the low signal levels involved and the difficulty of maintaining a very stable level of radiofrequency power it is advantageous to *traverse the whole resonance curve* in a relatively short time. This can be achieved either by "sweeping" the frequency of the radiofrequency oscillator while maintaining the magnetic field constant, or by "sweeping" the magnetic field while the frequency remains fixed. In early NMR experiments as well as in this laboratory the choice is to sweep the field with a pair of Helmholtz coils,[17] as indicated in Fig. 7.7a, because it is easy and does not require fancy frequency generators. The sweep coils are fed with a slowly varying current,[18] which results in a modulation of the magnetic field B. If this sweep covers the value of B_0, which is in resonance with the fixed frequency of the oscillator, a resonance signal modulated at the frequency of

[17] A pair of coils of diameter d, spaced a distance $d/2$ apart and traversed by current in the same direction, produce a very homogeneous field at the geometrical center of the configuration.

[18] In the absence of a sweep generator and audio amplifier the 60-Hz line voltage can be used through a variac and an isolation transformer.

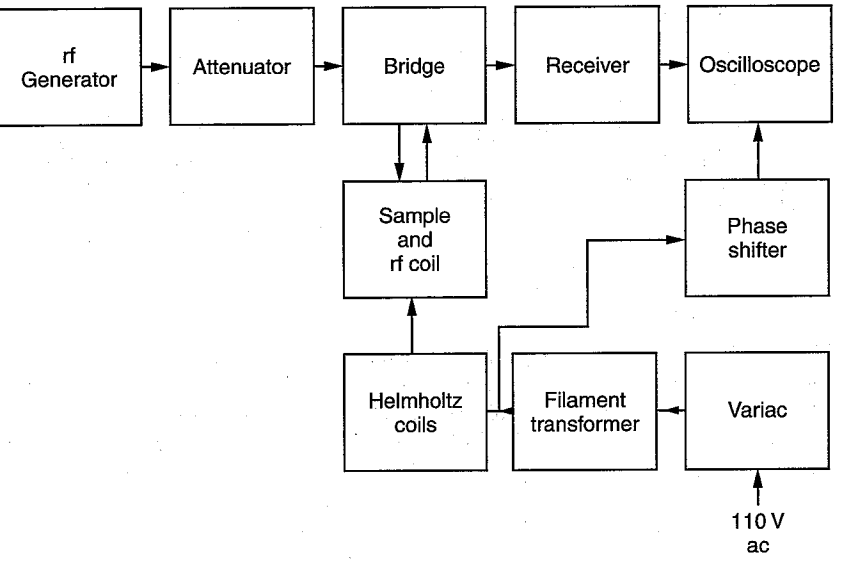

FIGURE 7.8 Block diagram of the nuclear resonance measuring apparatus.

ne sweep will appear at the detector. A modulated signal has the advantage f easier amplification and improvement in the signal-to-noise ratio by sing a narrow bandwidth detector.

The radiofrequency oscillator and detection circuit can be of several esigns. Today, commercial frequency generators are used to provide he RF drive and low-noise amplifiers for the detector. A *single* coil is sed as both a transmitter and receiver. A block diagram of a CW NMR pparatus as used in this laboratory is shown in Fig. 7.8. The signal vas detected by a bridge circuit; this arrangement has great sensitivity ut can be used without retuning only over a fairly narrow frequency ange.

Commercial magnetometers often use a "marginal oscillator" circuit vhere the oscillator and detector are combined in one unit. In this design he RF power is kept low so as to allow the direct observation of the bsorption, as well as to avoid saturation of the sample. To cover a wide requency range the coil containing the sample is changed since it is part f the resonant circuit that sets the oscillator frequency. A unit suitable for aboratory demonstrations is available from Klinger Educational Products, s well as from other sources.

7.4.2. Detection of Nuclear Magnetic Resonance with a Bridge Circuit

The coil in which the sample is located is part of a resonant circuit with high Q. The Q value, or quality factor, of a device is defined as 2π times the ratio of the time-averaged energy stored to energy dissipated, in one cycle. For a coil of inductance L and resistance R,

$$Q = \frac{2\pi\omega L}{R}. \tag{7.43}$$

When resonance is reached, the real part of the magnetic susceptibility (Eq. (7.35)) changes, and thus the inductance of the coil also changes. Alternatively, an increase in the imaginary part of the susceptibility (Eq. (7.36)) corresponds to the absorption of power from the field and thus to increased dissipation and therefore increased resistivity of the coil. This small change in the Q value can be detected with a bridge circuit, as shown in Fig. 7.9.

The radiofrequency voltage is applied between points a and g (see Fig. 7.9a), and therefore radiofrequency current flows through the load L and the dummy branch D; if the bridge is balanced, no voltage should appear at the point d (since b and c were in phase and of the same amplitude, and the signal from c and d is shifted by $\lambda/2$). Any slight unbalance of the bridge produces a small voltage at d. The actual bridge circuit is shown in (b) of the figure. The $R'C'$ elements are effectively generating

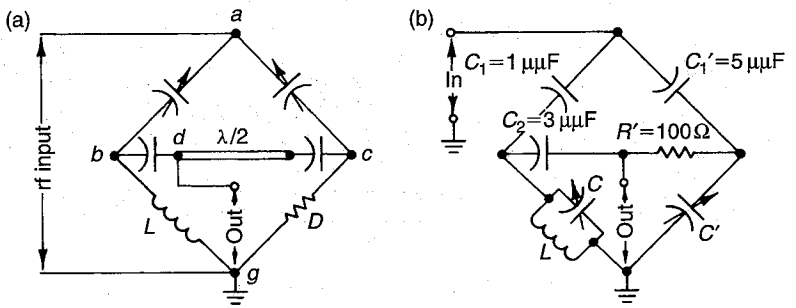

FIGURE 7.9 A radiofrequency bridge circuit that can be used for the detection of nuclear magnetic resonance. (a) Schematic arrangement; note that L is the radiofrequency coil. The $\lambda/2$ line ascertains cancellation at the output of the signals from b and c. (b) A practical radiofrequency bridge circuit. For resonance conditions see Eqs. (7.44) of the text.

the $\lambda/2$ phase shift and L is the sample coil. The conditions for balance are

$$\begin{aligned} &\text{Resistive balance:} && \omega^2 C_1 C_2 \left(1 + C'/C_1'\right) R' R_p = 1 \\ &\text{Reactive balance:} && C + C_1 + C_2 \left(1 + C_1/C_1'\right) = 1/L\omega^2, \end{aligned} \tag{7.44}$$

where R_p is the parallel resistance of the coil. The bridge is balanced either in the resistive mode, when the change in the Q of the coil will appear as an absorption curve as in Fig. 7.5b, or the bridge may be balanced in the reactive mode, when the signal appears as a dispersion curve as in Fig. 7.5a.

The experimental results obtained with this arrangement by a student are shown in Fig. 7.10. The sample was 1 cm^3 of water doped with manganese nitrate [$Mn(NO_3)_2$]. In Fig. 7.10a the bridge was balanced in the reactive mode, whereas in Fig. 7.10b it was balanced resistively. The sweep, derived from the 60-Hz line voltage, corresponds to approximately 10^{-4} T/division at the center of the oscilloscope trace.

The exact frequency at resonance can be measured quite precisely with a (crystal-controlled) "wave meter" to better than 1 part in 10^6. The magnetic field is measured either with a Hall probe magnetometer or with a rotating coil flux-meter.

From the experimental curves of Fig. 7.10 it is found that the frequency at resonance is

$$\nu_0 = 28{,}141.48 \pm 0.63 \text{ kHz}.$$

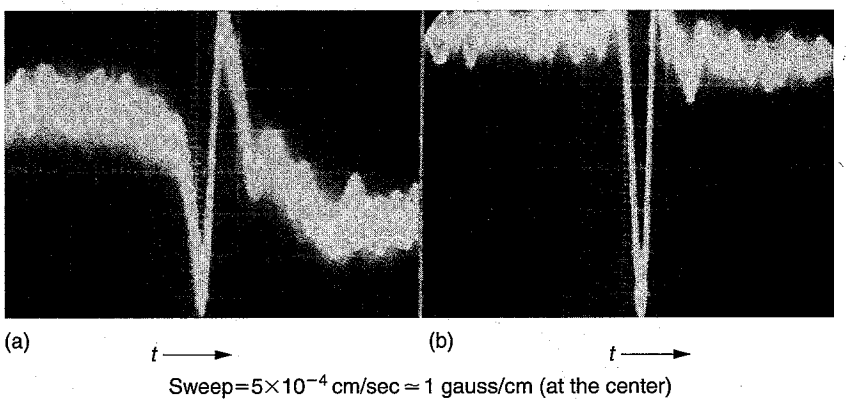

FIGURE 7.10 Results obtained from the nuclear magnetic resonance of protons using a bridge circuit: (a) Dispersion curve and (b) absorption curve. The oscilloscope sweep was linear at 0.5 ms/cm, which corresponds to approximately 10^{-4} T/cm at the center of the sweep.

Using a rotating coil flux-meter at the field position previously occupied by the sample, the magnetic field at resonance is found to be

$$B_0 = 0.6642 \pm 0.0020 \text{ T},$$

and hence

$$\gamma = \frac{2\pi\nu_0}{B_0} = (26.618 \pm 0.08) \times 10^7 \text{ rad/s-T} \tag{7.45}$$

in good agreement with the accepted value

$$\gamma = 26.73 \times 10^7 \text{ rad/s-T}.$$

Clearly, it is much easier to measure ratios of nuclear moments to high accuracy than to establish their absolute value to the same accuracy.

To obtain the g factor of the proton—that is, the connection between magnetic moment and the nuclear magneton—we recall that

$$\mu = gI\mu_N.$$

Thus from Eq. (7.4)

$$g = \frac{\gamma\hbar}{\mu_N} = \frac{\gamma}{2\pi}\frac{1}{\mu_N/h} = 5.56 \pm 0.02,$$

where we used the derived value of γ (Eq. (7.45)) and μ_N/h from Eq. (7.2). We have measured the proton magnetic moment of the proton to an accuracy of 0.4%.

7.4.3. Measurement of T_2^*

In this laboratory no pulsed NMR experiments were carried out. However, under certain conditions one can observe the free induction and its decay with a CW apparatus. This happens if the field is swept rapidly enough through the resonance, in which case wiggles such as those shown in Fig. 7.11 appear.

The interpretation follows the discussion of Section 7.3.4. Far from resonance the field seen in the rotating frame is B_0, i.e., along the z axis. As resonance is approached the B_0 field is canceled in the rotating frame and only H_1 is present. This results in rotating the **M** vector into the x'–y' plane. After the resonance is traversed the effect of H_1 is again minimal, but the magnetization remains in the x'–y' plane, and it induces a signal at

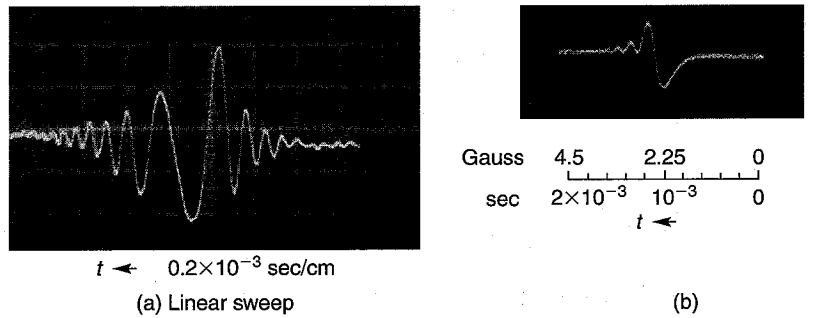

FIGURE 7.11 Nuclear magnetic resonance signals of protons obtained with a marginal oscillator circuit. (a) The sample is water-saturated with LiF. (b) The sample is water-doped with manganese nitrate. A linear sweep of the same speed is used in both cases.

a frequency $\omega(t) = \gamma B_0(t)$, which differs from ω_0. The two frequencies $\omega(t)$ and ω_0 beat against each other, and this gives rise to the wiggles. One can clearly see that the frequency difference increases (the beating period shortens) as the field is further away from resonance. The effect that is relevant for our measurement is the exponential decay of the envelope of the beat oscillations.

We still must explain the wiggles that appear in Fig. 7.11a before the resonance is crossed. These are present because the spins have not dephased by the time the sweep is restarted and continue to rotate in the x–y plane. Indeed they are absent from the trace of Fig. 7.11b where the water sample was doped with manganese nitrate as compared to water-doped with LiF in the sample used for Fig. 7.11a. The shorter T_2 in part (b) of the figure leads to more rapid dephasing.

If a linear sweep is assumed, the beat signal has the form

$$e^{-t/T_2^*} \cos\left[\frac{1}{2}\gamma \frac{dH}{dt} t^2\right], \tag{7.46}$$

where $t = 0$ when the resonance is traversed. Note also that the beat frequency increases with time since

$$\omega_b = \frac{1}{2}\gamma \frac{dH}{dt} t.$$

From a measurement of the wiggle envelope, information about T_2^* can be obtained. This is shown in Fig. 7.12 where the data are well fitted by an

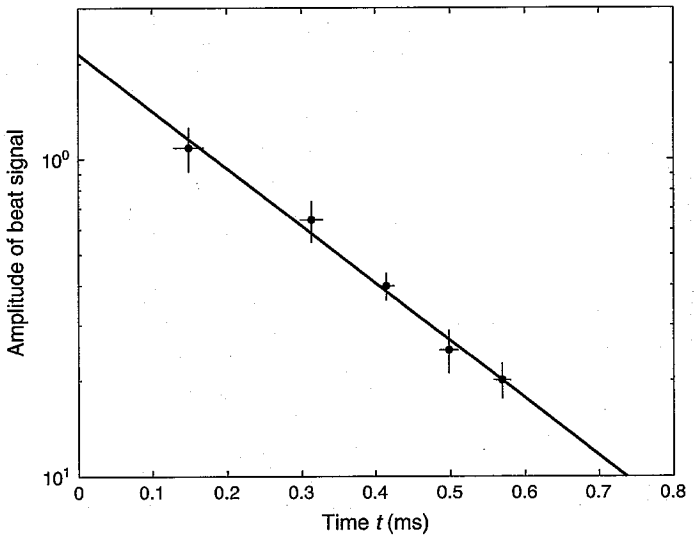

FIGURE 7.12 Semilog plot of the amplitude of the "wiggles" of the resonance signal shown in Fig. 7.11a plotted against time. It yields an exponential decay of the amplitude with a time constant $T_2^* = 2.4 \times 10^{-4}$ s.

exponential yielding

$$T_2^* = 2.4 \times 10^{-4} \text{ s}.$$

When we convert the measured value of T_2^* into a magnetic field (see Eq. (7.37)), we find that

$$2\Delta B_0 = \frac{2}{T_2^* \gamma} = 3.2 \times 10^{-5} \text{ T},$$

namely, that an inhomogeneity of the magnetic field, over the size of the sample, of 0.32 G is sufficient to cause the wiggles observed in Fig. 7.11a. We also conclude that T_2 for this sample is longer than 2.4×10^{-4}s.

7.4.4. The Effect of T_1

In Fig. 7.13 we show a very simple marginal oscillator circuit[19] that is adequate for demonstrating NMR signals. The first transistor supplies constant

[19] J. R. Singer and S. D. Johnson, *Rev. Sci. Instrum.*, **30**, 92 (1959).

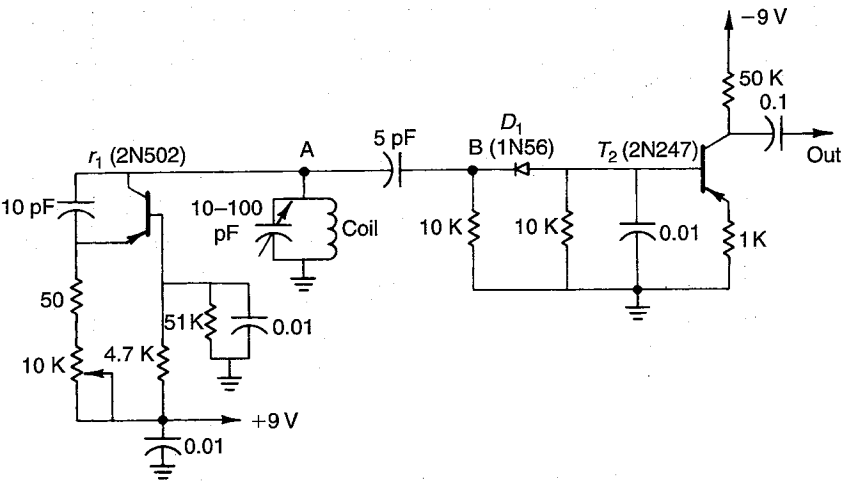

FIGURE 7.13 A simple transistorized nuclear magnetic resonance circuit.

current to the coil attached to point A. Any change in the Q of the coil appears as a change in voltage at that point, which is then amplified by the output transistor. The circuit will oscillate in the range of 2–80 MHz, depending on the resonance set by the coil LC circuit.

Data obtained by a student using a 1-cm^3 sample of water doped with manganese nitrate are shown as a function of RF amplitude in Fig. 7.14. The amplitude is controlled by the 10-kΩ potentiometer in the oscillator loop of the circuit of Fig. 7.13. The data were obtained in a field $B_0 = 0.8$ T ($\nu_0 = 33.83$ MHz). The RF level as measured across the coil is indicated for each of the traces shown in the figure. Note that the NMR signal increases with increasing RF power until the RF amplitude reaches approximately 0.5 V. Beyond this point the signal decreases because the sample is saturated. From a knowledge of the Q of the coil one can convert the RF amplitude to the corresponding value of the rotating field H_1 and thus use the data to find the spin–lattice relaxation time T_1.

Note also that once the sample is saturated there is sufficient magnetization left in the x–y plane to begin showing a beat signal (wiggles) after passage through resonance (see Fig. 7.11b). For convenience the time scale on the oscilloscope trace in Fig. 7.14 was set to cover a full cycle of the 60-Hz sinusoidal sweep.

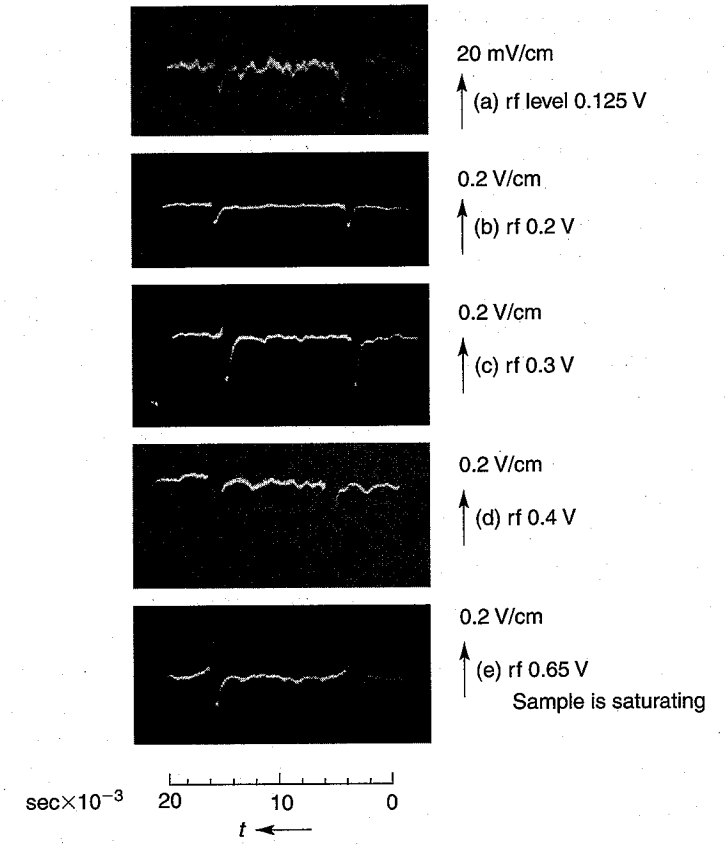

FIGURE 7.14 Nuclear magnetic resonance signals from protons obtained with the circuit shown in Fig. 7.13 as a function of the amplitude of the radiofrequency. Note that initially the output signal increases with increasing radiofrequency amplitude but at a level of approximately 0.5 V the sample is saturated and the signal begins to decrease. The signal of 0.5 V is shown in Fig. 7.11b.

7.5. ELECTRON SPIN RESONANCE

7.5.1. General Considerations

So far we have discussed transitions between the energy levels of a proton or a nucleus in the presence of an external magnetic field. Transitions between the energy levels of a quasi-free electron in an external magnetic field can also be observed. We refer to this case as *electron spin resonance* (ESR)